THE ASTROPHYSICAL JOURNAL, 322:559–572, 1987 November 1

CLOUD CHEMISTRY ON JUPITER

BARBARA E. CARLSON, MICHAEL J. PRATHER, AND WILLIAM B. ROSSOW
NASA/Goddard Space Flight Center, Institute for Space Studies
Received 1987 March 6; accepted 1987 April 22

ABSTRACT

Chemical equilibrium models have been used to interpret observations and constrain models of Jupiter. We reexamine the chemical reactions controlling the composition of the cloud-forming region from 10 to 0.1 bar and the thermodynamic data used in these models. Aqueous reactions decrease the abundances of NH_3 and H_2S; these reactions prevent the transport of CO_2 from deeper levels, with little or no effect on the abundances of CO or weakly basic species such as PH_3. Formation of NH_4SH rapidly removes most of the H_2S, while for a solar N/S ratio the NH_3 abundance decreases by only 20%. If, as suggested by de Pater, the H_2S abundance is enhanced by a factor of 5, formation of NH_4SH would deplete NH_3 by as much as 70% and still be consistent with the observations. Measurements of near solar abundances of NH_3 in the 1 bar region require enhanced abundances at depth to offset depletions due to chemical reactions in the clouds. Best agreement with the observations is found for 2 times solar abundances of N, O, and S relative to H.

Subject headings: molecular processes — planets: atmospheres — planets: Jupiter

I. INTRODUCTION

Thermochemical equilibrium models have been constructed for the Jovian atmosphere based on the assumptions of solar composition, an adiabatic temperature profile, and hydrostatic equilibrium. These models can be used to predict the vertical distributions of the photochemically stable compounds and the location of cloud bases. Two primary studies (Lewis 1969, henceforth L69; Weidenschilling and Lewis 1973, henceforth WL73) predicted that, as temperature decreases with altitude from 400 K, H_2O would be the first species to condense, followed by NH_4SH, and then by NH_3. Measurements from ground and from spacecraft have sustained aspects of these thermochemical models.

We use new data defining thermal profiles which are substantially different from those used in L69 and WL73. Recent analyses which use these new thermal profiles have resorted to scaling the results of WL73 to account for differences in temperature or chemical abundances (West, Strobel, and Tomasko 1986); however, the chemical model has not been critically reviewed. We present a model for the chemical reactions controlling the composition of the upper troposphere on Jupiter, specifically the cloud-forming region from 10 bar to 0.1 bar.

We correctly include, for the first time, the effects of aqueous chemistry on the composition and vertical distribution of many measurable species in the atmosphere, identifying the factors influencing their abundances above the H_2O cloud. We critically reexamine the thermodynamic data for potential condensates on Jupiter, NH_3(s), NH_4SH(s), $(NH_4)_2S$(s) and H_2S(s), recognizing the lack of data on sulfides for the temperature range of interest on Jupiter. In order to be consistent with available spectroscopic measurements, the bulk abundances of N, O, S, and P with respect to H are likely to be at least 2 times the solar abundance, as is currently observed for C as CH_4 in the upper troposphere.

The observational constraints on the atmospheric structure and composition of Jupiter are reviewed in § II. The thermochemical model is described in § III, and the results in § IV. A summary of the preferred composition is given in § V with the observational consequences outlined in § VI.

II. ATMOSPHERIC STRUCTURE AND COMPOSITION

Recent observations and reanalysis of earlier data suggest that the pressure-temperature (*P-T*) profile in the Jovian atmosphere is substantially different from those used by L69 and WL73. Figure 1 compares the *P-T* profiles used in these studies with a profile derived by Orton (1981). The more recent profile is based on an average of the *Voyager* radio subsystem (RSS) occultation experiment results (Lindal *et al.* 1981), obtained for several locations in the neutral atmosphere using the bulk composition determined by Gautier *et al.* (1981). Use of this new *P-T* profile shifts the location of the cloud bases to lower pressures as compared to L69 and WL73, as the clouds form at roughly the same temperatures.

Determination of the trace gas abundances in the Jovian atmosphere by remote sensing is complicated by a number of factors. First, the depth to which remote observations are able to penetrate the Jovian atmosphere is a function of wavelength, since both cloud and gas opacities vary strongly with wavelength. Current studies of gas abundances generally do not include the spectral dependence of the cloud opacity. Even in regions of minimum opacity (i.e., "spectroscopic windows"), remote-sensing techniques are limited by cloud and gas opacities to roughly the upper 6 bars of the atmosphere. Second, the retrieval of a gas abundance from an absorption spectrum requires knowledge of the pressure-temperature profile, as well as the vertical distribution of the gaseous absorber. Due to low vapor pressures, low solubilities in liquid water, and long photochemical lifetimes in the troposphere, the gases H_2, He, and CH_4 are expected to maintain a constant mixing ratio within the troposphere. This is not the case for condensable and chemically reactive species for which the mixing ratio can vary rapidly with altitude.

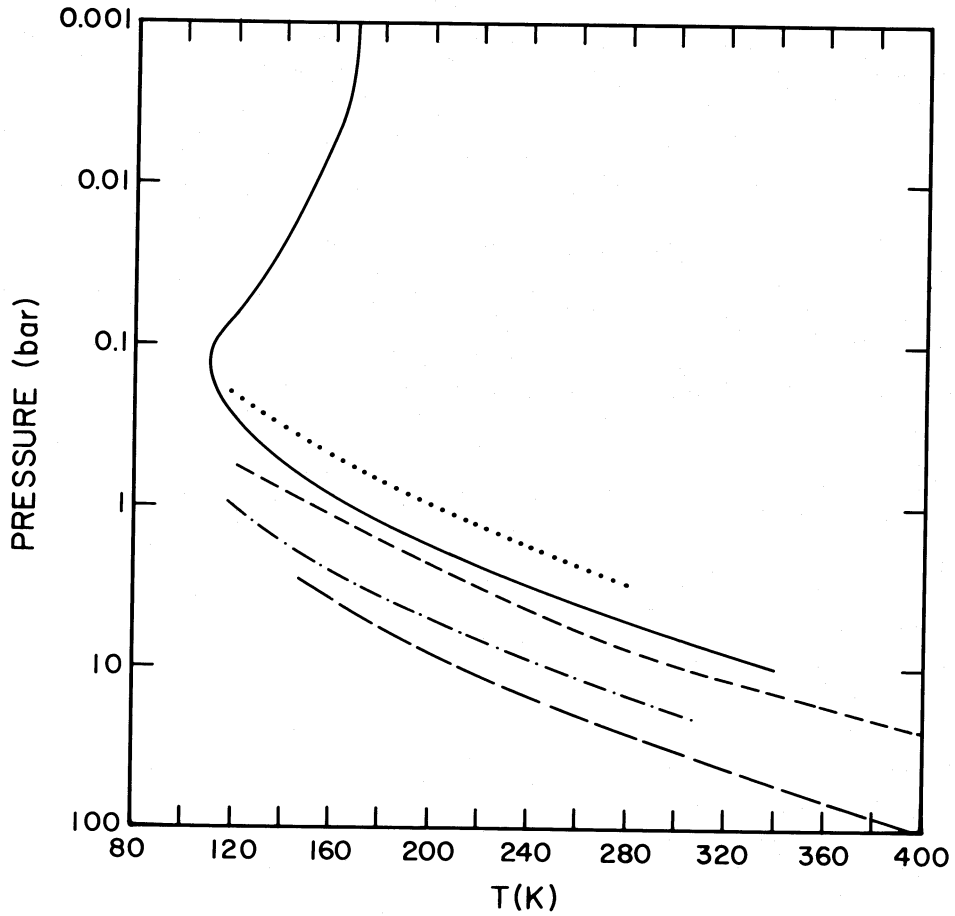

FIG. 1.—Pressure-temperature profiles for Jupiter. The solid line denotes the profile used in this investigation (Orton 1981). Profiles used by Weidenschilling and Lewis (1973) are indicated: profile **a** (*dotted line*), **b** (*short dashes*), and **c** (*dash-dot*). Profile **b** of Lewis (1969) is also shown (*long dashes*).

Table 1 lists the solar elemental abundances relative to H_2 for some of the cosmically most abundant elements (Cameron 1982). Analysis of the *Voyager* IRIS data gives an H_2 mole fraction of 0.897 ± 0.030, which implies a helium mass fraction of 0.19 ± 0.05 (Gautier *et al.* 1981). The fully reduced forms of O, C, N, and S in the Jovian atmosphere are H_2O, CH_4, NH_3, and H_2S; these compounds are expected to be the predominant form of these elements in the upper troposphere.

a) Carbon

For a well-mixed gas such as methane, abundance determinations based on analyses of spacecraft and ground-based data at a variety of wavelengths are in good agreement. The original value derived by Gautier *et al.* (1982) from the thermal infrared *Voyager* IRIS spectra of the North Equatorial Belt (NEB) $(1.95 \pm 0.22) \times 10^{-3}$ has been revised $(2.18 \pm 0.18) \times 10^{-3}$ (Gautier and Owen 1983). This range of CH_4 abundance is consistent with earlier determinations from ground-based observations in the visible $(1.8 \pm 0.4) \times 10^{-3}$ (Sato and Hansen 1979) and near-infrared at 1.1 μm $(2.6 \pm 1.2) \times 10^{-3}$ (Buriez and de Burgh 1980). Recently, Bjoraker, Larson, and Kunde (1986*a*) reported the first detection of the weak ν_3–ν_4 hot band of CH_4 in Jupiter's 5 μm spectrum. From this they were able to infer a mixing ratio for methane in the deep troposphere of $(3.0 \pm 1.0) \times 10^{-3}$, corresponding to a C/H ratio which is 3.6 ± 1.2 times solar. This range is marginally consistent with the other values and points to difficulties in interpreting 5 μm spectra (see discussion of H_2O below), even for a well-mixed species such as methane.

Other carbon compounds observed in the Jovian atmosphere include CO (Beer 1975) and nonmethane hydrocarbons such as C_2H_2 and C_2H_6 (Ridgway 1974). The presence of an oxidized carbon species, CO, has been explained as a result of mixing of this locally unstable species from deeper regions of the atmosphere where the compound is thermochemically stable (Prinn and Barshay 1977). Alternative explanations (Prather, Logan, and McElroy 1978; Strobel and Yung 1979) suggest that the presence of CO in the upper atmosphere is the result of photochemical reactions involving an extraplanetary source of oxygen.

TABLE 1

RATIOS RELATIVE TO H_2

Element	Abundance
H_2	1
He	1.35×10^{-1}
O	1.38×10^{-3}
C	8.35×10^{-4}
N	1.74×10^{-4}
S	3.76×10^{-5}
P	4.89×10^{-7}

a Solar composition based on Cameron (1982).

New observations suggest that CO is well-mixed throughout the troposphere with a mixing ratio of at least 10^{-9} (Bjoraker, Larson, and Kunde 1986*a*; Noll *et al.* 1987*a*, *b*). This finding requires a CO source from the deep atmosphere in addition to any stratospheric component. Such a large abundance of CO in the troposphere also has important implications regarding the bulk composition of the atmosphere. If the relative abundance of oxygen were solar or less, mixing ratios for CO greater than 10^{-9} are in thermochemical equilibrium only for $T > 1000$ K (Prinn and Barshay 1977). Since chemical kinetic conversion of CO to CH_4 proceeds efficiently near 1000 K (Prinn and Barshay 1977), the abundance of CO reaching the upper troposphere would be reduced to less than 10^{-9}, provided the vertical eddy diffusion coefficient is no larger than 10^4 m^2 s^{-1} as assumed by Prinn and Barshay. If the oxygen abundance were supersolar by a modest factor, the abundance of CO would be as large as 10^{-9} in the region of rapid equilibration near 1000 K. We examine the efficiency of transport of CO and CO_2 (another possible source of CO) from the deep atmosphere through the water cloud layer.

b) Nitrogen

Observed abundances of NH_3 are summarized in Figure 2. The inferred values for the mixing ratio of NH_3 depend upon which wavelength, and hence, which region of the atmosphere, is observed. For example, Sato and Hansen (1979) conclude from their analysis of reflected solar radiation that the NH_3 mixing ratio is $(2.8 \pm 1.0) \times 10^{-4}$ or 1.5 ± 0.5 times the solar ratio at the 1 bar level. This is consistent with the value $(1.78 \pm 0.89) \times 10^{-4}$ determined by Kunde *et al.* (1982) for the 1 bar level from their analysis of *Voyager* IRIS spectra from the NEB. Kunde *et al.* further conclude that the NH_3 mixing

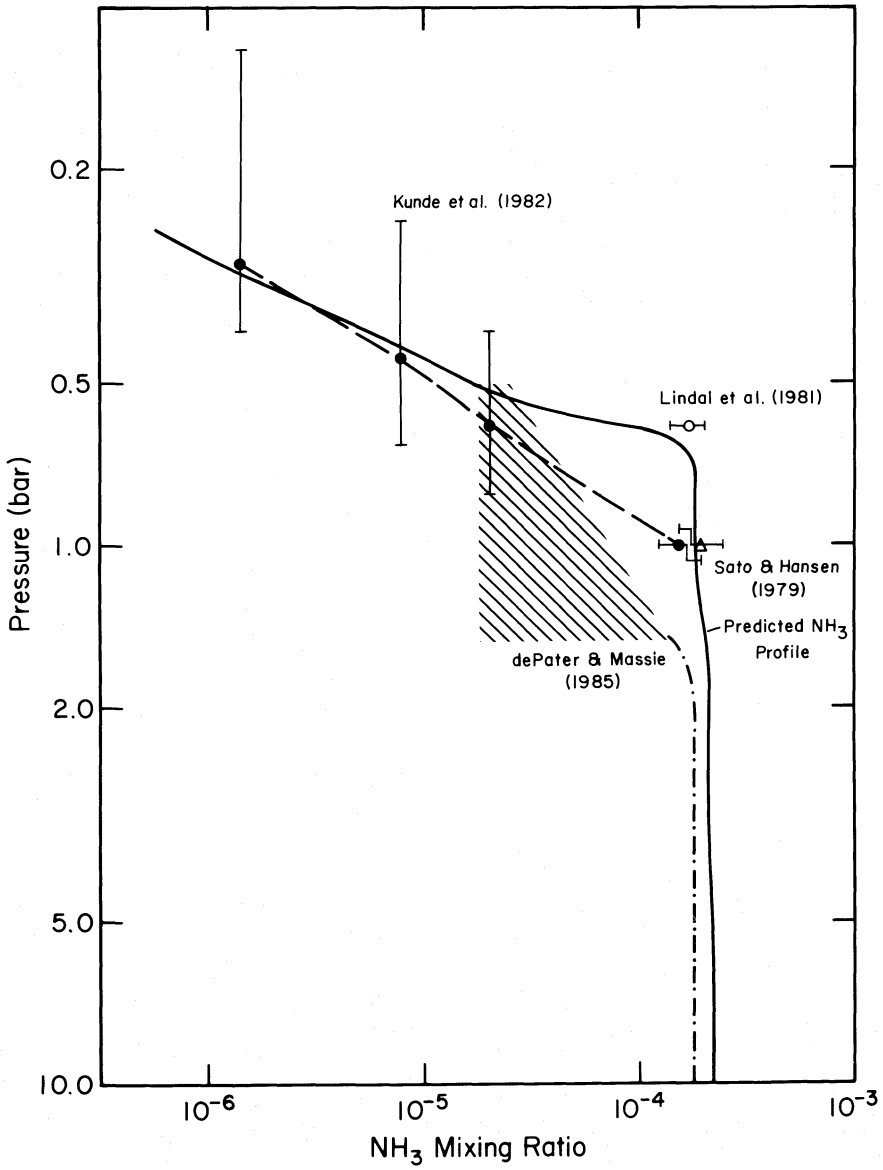

FIG. 2.—Vertical profiles of the NH_3 mixing ratio. Model results for the case of 2 times solar are indicated by the solid line. Values for the NH_3 mixing ratio are reported by Sato and Hansen (1979, *open triangle*) and Kunde *et al.* (1982, *filled circles*). Abundances inferred from the RSS data (Lindal *et al.* 1981, *open circle*) correspond to supersaturated values. The profile retrieved by de Pater and Massie (1985, *hatched area plus dash-dot line*) suggests subsaturated abundances.

ratio decreases by a factor of 3 between 1.0 and 0.7 bar. Ground-based observations at millimeter and centimeter wavelengths, on the other hand, have led de Pater and Massie (1985) to conclude that the NH_3 mixing ratio is (3.0–3.8) $\times 10^{-5}$ in the region, $0.5 < P < 1.0$–1.5 bar, and is a factor of 4–5 smaller than the solar value. The depletion of NH_3 inferred by de Pater and Massie, as shown in Figure 2, also conflicts with the analysis of the *Voyager* RSS occultation (Lindal *et al.* 1981), which implies an ammonia abundance of $(2.2 \pm 0.8) \times 10^{-4}$ near the 0.6 bar level. It is clear from the *Voyager* IRIS results (Kunde *et al.* 1982; Gierasch, Conrath, and Magalhaes 1986) and from the analyses of ground-based data (Moroz and Cruikshank 1969) that NH_3 varies with altitude and location, making it difficult to determine the bulk abundance of NH_3 in the Jovian atmosphere.

Thermochemical and photochemical models for NH_3 in the Jovian atmosphere predict that NH_3 should condense in the upper troposphere (WL73) and above that be subject to a substantial amount of photochemical destruction in the stratosphere and upper troposphere (Strobel 1973). Furthermore, the interaction of microphysical and dynamical processes in the cloud can alter the vertical NH_3 profile, reducing the mixing ratio to subsaturated levels (Carlson, Rossow, and Orton 1987). A first-order model for the altitude dependence of NH_3 vapor is to assume a constant mixing ratio up to the location of the cloud base (i.e., the saturation level) and then allow the vapor profile above this level to follow the saturation vapor pressure. While this approach is an improvement over the assumption of a well-mixed profile used in some spectroscopic studies, substantial deviations from this uniform model are expected and observed (Gierasch, Conrath, and Magalhaes 1986). In particular, the NH_3 abundance at NH_3 cloud levels will be affected by the formation of an ammonium hydrosulfide condensate near the 2 bar level (see § II*d*), and formation of an aqueous solution in the water cloud region of 4–5 bar. Thus the mixing ratio of NH_3 is expected to decrease with altitude over the entire extent of the observable atmosphere from the base of the water cloud to the stratosphere.

c) Oxygen

Based on thermochemical considerations, the base of the water cloud for a Jovian atmosphere with a solar abundance of oxygen should be located near 4.8 bar (275 K). This region of the atmosphere may be just within the limits of current capabilities in remote sensing depending on the opacities of the cloud layers, but most observations will probably refer to the region above the cloud. The abundance of water within the Jovian atmosphere has been derived from aircraft data at 2.7 μm (Larson *et al.* 1984), *Voyager* IRIS data in the 5 μm region (Kunde *et al.* 1982), and a combination of *Voyager* IRIS and aircraft data in the 5 μm region (Bjoraker 1985; Bjoraker, Larson, and Kunde 1986*b*). These abundance observations are shown in Figure 3. Kunde *et al.* (1982) obtain a profile for the mixing ratio of H_2O varying from 3×10^{-5} at 4 bar to 1×10^{-6} at 2.5 bar, while Bjoraker, Larson, and Kunde (1986*b*) find a similar variation but attribute it to levels deeper than 4 bar. Bjoraker, Larson, and Kunde (1986*b*) point out, however, that the location of the levels to which the results apply is dependent on the radiative model used in the analysis. Kunde *et al.* assume the presence of a gray, absorbing haze with a total optical depth of 0.54 at 5 bar uniformly mixed throughout the line-forming region (1–5 bar) and an optically thick lower boundary at 279 K, whereas Bjoraker, Larson, and Kunde (1986*b*) assume the presence of a gray cloud above the line-forming region at 210 K ($\sim$2 bar) with an optical depth of 2.93 and an optically thick lower boundary at 353 K ($\sim$12 bar). One factor not considered is that Bjoraker, Larson and Kunde (1986*b*) use a Lorentz line profile truncated at 50 cm^{-1} from line center, whereas Kunde *et al.* extend the lines to 250 cm^{-1}. These differences in model boundary conditions, line profiles, and cloud opacities and locations lead to the differences shown in Figure 3 in the H_2O distributions inferred from the same data.

Bjoraker, Larson, and Kunde (1986*b*) note that the retrieved H_2O abundances suggest the formation of an ice cloud above the 2 bar level, yet the radiative transfer models used in these retrievals do not include the spectrally dependent absorption associated with ice clouds of either NH_3 (Martonchik, Orton, and Appleby 1984) or H_2O (Schaaf and Williams 1973). Kunde *et al.* (1982) have demonstrated that the presence of even a gray haze, distributed throughout the line-forming region (1–5 bar), will alter the shape of the continuum (cf. Fig. 15 of their paper). The observed continuum spectrum, against which the predicted H_2O(g) absorption is compared, will be lower than expected as all sources of opacity have not been included (e.g., water ice). The analysis of line-to-continuum ratios may underestimate the amount of gas required to reproduce the depth of the absorption features in the spectra. Even in the case of a pure gas atmosphere there are difficulties in the analysis of H_2O observations: for the two recent studies (Kunde *et al.* 1982; Bjoraker, Larson, and Kunde 1986*a*, *b*) we note a difference of 2 bar in the pressure level at unit optical depth. Pressure levels for the cores of selected H_2O lines (Bjoraker, Larson, and Kunde 1986*b*) are assigned on the basis of gas opacity only and do not include the extinction due to aerosol scattering or absorption. If aerosol extinction is significant, the inferred pressure associated with unit optical depth would be reduced.

Bjoraker, Larson, and Kunde (1986*b*) do not consider a self-consistent case with a solar O/H abundance. For their "solar" case, they increase the O/H ratio to solar without moving the lower boundary of their radiative transfer model from 12 bar (353 K) up to 5 bar (279 K) which is necessary to account for the presence of an optically thick water cloud as required by the H_2O abundance. Bjoraker (1985) alters the lower boundary condition of the radiative model without changing the O/H ratio. A complete, consistent analysis of the "solar" case is needed before we abandon the logical assumption of a solar O/H ratio. A solar abundance of O is also supported by the observations of CO. We therefore choose to interpret the abundances determined from these studies as a lower limit to the bulk abundance of water on Jupiter.

d) Sulfur

Hydrogen sulfide is presumably the main sulfur-bearing compound in the deep Jovian atmosphere. The failure to detect H_2S above the visible clouds has been interpreted as an upper limit on the bulk elemental ratio S/H of 1.7×10^{-8} (Larson *et al.* 1984). More likely, this upper limit of $(2.1–3.3) \times 10^{-8}$ to the H_2S abundance in the region, 0.75–1.2 bar, may be explained by chemical reactions, such as the gas phase reaction with NH_3 to form NH_4SH(s), which reduce the observed abundance relative to the (presumably) solar abundance of S in the deep atmosphere (Larson *et al.* 1984). One study based on millimeter-wave spectra (Bézard *et al.* 1983), however, infers a higher, near solar mixing ratio of H_2S at pressures greater than 1 bar; but this interpretation is ambiguous (cf. West, Strobel,

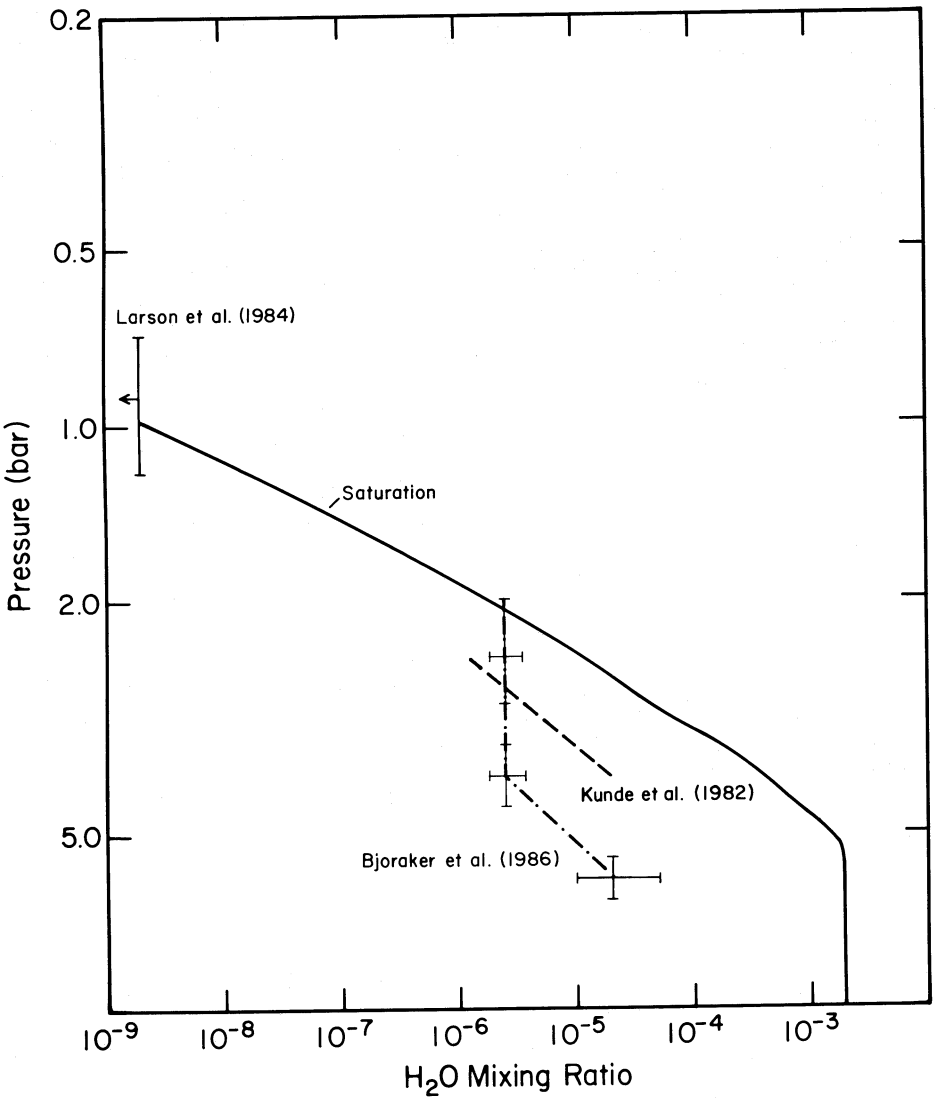

FIG. 3.—Vertical profiles of the H_2O mixing ratio. Model results for the case of 2 times solar are indicated by the solid line. Values from Larson *et al.* (1984) are shown as a strict upper limit at 1.2 bar. Profiles retrieved from 5 μm observations (Kunde *et al.* 1982, *dashes*; Bjoraker, Larson, and Kunde 1986*b*, *dash-dot*) disagree. Error bars are indicated for the Bjoraker, Larson, and Kunde (1986*b*) profile.

and Tomasko 1986). More recently, de Pater (1986) has interpreted the depletion of NH_3 observed at radio wavelengths to be an indication of a nonsolar N/S ratio with an S/H ratio of 10 times solar. One may conclude either that the Jovian abundance of sulfur is extremely subsolar or that chemical reactions within the atmosphere are effective in reducing the abundance of H_2S. In the next sections, we examine the properties of NH_4SH(s), and other sulfide condensates, H_2S(s) and $(NH_4)_2S$(s), as well as considering the aqueous chemistry of H_2S. We show that uncertainties in the thermodynamic properties of NH_4SH(s) include a range of altitudes for the cloud base but do not alter the major effect: removal of most of the H_2S from the observable regions of the atmosphere.

III. THERMOCHEMICAL MODEL

a) Reactions

We present a thermochemical model for the upper troposphere of Jupiter in which chemical reaction rates are assumed to be in equilibrium at a fixed P and T. Condensation is modeled through the following chemical reactions:

$$H_2O(g) \Leftrightarrow H_2O(l) \quad (1)$$

$$H_2O(g) \Leftrightarrow H_2O(s) \quad (2)$$

$$NH_3(g) \Leftrightarrow NH_3(s) \quad (3)$$

$$NH_3(g) + H_2S(g) \Leftrightarrow NH_4SH(s) \quad (4)$$

$$H_2S(g) \Leftrightarrow H_2S(s) \quad (5)$$

and under conditions of high partial pressures of NH_3 (Magnusson 1907),

$$2NH_3(g) + H_2S(g) \Leftrightarrow (NH_4)_2S(s) \quad (6)$$

Reactions (1)–(4) were included in L69 and WL73.

For the condensates we use Raoult's law given by

$$P_i = Kx_i \quad (7)$$

to determine the partial pressure P_i (atm) of species i in equilibrium with the solid phase, where K is the equilibrium coeffi-

cient and x_i is the mole fraction. For the condensates x_i is unity except in the case of liquid water with a substantial quantity of dissolved material for which $x_i < 1$. The equilibrium coefficient is calculated from

$$\ln K = +\Delta G/RT , \quad (8)$$

where ΔG is the change in Gibbs free energy for the forward reaction as given in Table 2, R the gas constant, and T the temperature in kelvins.

The following reactions describe gases dissolved in liquid water (i.e., aqueous phase):

$$CH_4(g) \Leftrightarrow CH_4(a) \quad (9)$$

$$NH_3(g) \Leftrightarrow NH_3(a) \quad (10)$$

$$H_2S(g) \Leftrightarrow H_2S(a) \quad (11)$$

and

$$CO_2(g) + H_2O(l) \Leftrightarrow H_2CO_3(a) . \quad (12)$$

For these calculations we assume that the gas is ideal and equate fugacity with partial pressure. Aqueous species are assumed to obey Henry's law

$$P_i = k_i[i] , \quad (13)$$

where P_i is the partial pressure (atm) of the gas i in equilibrium with its solution, k_i is Henry's coefficient, and $[i]$ denotes the concentration of species i in the solution (moles per liter of liquid water). Henry's coefficient is found from

$$\ln k_i = +\Delta G/RT . \quad (14)$$

Chemical reactions in the aqueous phase lead to dissociation of the dissolved gases (all ions are in the aqueous phase). We include the following reactions:

$$H_2O(l) \Leftrightarrow H^+ + OH^- \quad (15)$$

$$NH_3(a) + H^+ \Leftrightarrow NH_4^+ \quad (16)$$

$$H_2S(a) \Leftrightarrow H^+ + HS^- \quad (17)$$

$$HS^- \Leftrightarrow H^+ + S^= \quad (18)$$

$$H_2CO_3(a) \Leftrightarrow H^+ + HCO_3^- \quad (19)$$

$$HCO_3^- \Leftrightarrow H^+ + CO_3^= . \quad (20)$$

Table 2 summarizes the thermodynamic data for these reactions. The equilibrium coefficients involving ions are corrected for activity by using coefficients, f, from Debye-Huckel theory:

$$\log f = -Az^2 I^{1/2}/(1 + I^{1/2}) , \quad I < 0.1 , \quad (21)$$

where $A \sim 0.5(300/T)^{1.5}$, z is the ion charge and I is the ionic strength (see Stumm and Morgan 1981, p. 135).

b) *Thermodynamic Data*

The available thermodynamic data for NH_4SH(s) display significant discrepancies. Large differences are found in the values reported for the entropy of solid NH_4SH. Wagman *et al.* (1968) cite the value S = 97.34 J deg^{-1} mol^{-1} at 298.15 K without reference, while Kelley and King (1961) give S = 113.28 ± 8.36 J deg^{-1} mol^{-1}. National Bureau of Standards (NBS) publications preceding the Wagman *et al.* reference (e.g., Rossini *et al.* 1952) refer to Randall and White (1928, a personal communication referred to in the International Critical Tables), who in turn refer to Isambert (1881) and Walker and Lumsden (1897). The references in Kelley and King (1961) can also be traced back to Isambert (1881) and Walker and Lumsden (1897). Figure 4*a* shows the comparison between the thermodynamic data for reaction (4) and the early laboratory measurements of Isambert (1881, 1882) and Walker and Lumsden (1897). The range of values recommended by Kelley and King (1961) is denoted, and a curve corresponding to the Wagman *et al.* (1968) value is shown. We selected the value S = 115.57 J deg^{-1} mol^{-1}, corresponding to the solid line in Figure 4*a*, a best fit to the observations. Lewis's (1969) formula (given by eq. [22] below) is also shown for comparison. None of the above provides an acceptable fit to the early laboratory data.

Lewis (L69) derived his own formula for the equilibrium

TABLE 2

THERMODYNAMIC DATA AT 298.15 K[a]

Reaction	ΔH(kJ/mol)	ΔG(kJ/mol)	ΔS(J/mol-K)
$H_2O(g) \Rightarrow H_2O(l)$	−45.00	−8.57	−122.20
$H_2O(g) \Rightarrow H_2O(s)$	−51.25	−7.97	−145.17
$NH_3(g) \Rightarrow NH_3(s)$	−31.67	9.86	−139.29
$NH_3(g) + H_2S(g) \Rightarrow NH_4SH(s)$	−89.97	−0.38	−282.45
$H_2S(g) \Rightarrow H_2S(s)$		see text	
$CH_4(g) \Rightarrow CH_4(a)$	−14.24	16.36	−102.60
$H_2(g) \Rightarrow H_2(a)$	−4.18	17.57	−72.90
$NH_3(g) \Rightarrow NH_3(a)$	−34.61	−9.99	−82.39
$H_2S(g) \Rightarrow H_2S(a)$	−19.12	5.69	−83.10
$CO_2(g) + H_2O(l) \Rightarrow H_2CO_3(a)$	−20.37	8.35	−96.51
$H_2O(l) \Rightarrow H^+ + OH^-$	56.80	79.84	−77.27
$NH_3(a) + H^+ \Rightarrow NH_4^+$	−51.74	−52.74	3.47
$H_2S(a) \Rightarrow H^+ + HS^-$	22.11	40.45	−61.57
$HS^- \Rightarrow H^+ + S^=$	50.72	73.64	−76.61
$H_2CO_3(a) \Rightarrow H^+ + HCO_3^-$	7.70	36.40	−96.30
$HCO_3^- \Rightarrow H^+ + CO_3^=$	14.90	58.90	−147.60
$2NH_4^+ + S^= \Rightarrow (NH_4)_2S$	0.35	−0.21	0.71
$(NH_4)_2S + H_2S(g) \Rightarrow (NH_4)_2S_2 + H_2(g)$	32.64	39.17	−11.85

[a] Data have been compiled from the *Handbook of Chemistry and Physics* (1983), *International Critical Tables* (1928), Kelley and King (1961), Wagman *et al.* (1978), and Stull and Prophet (1971).

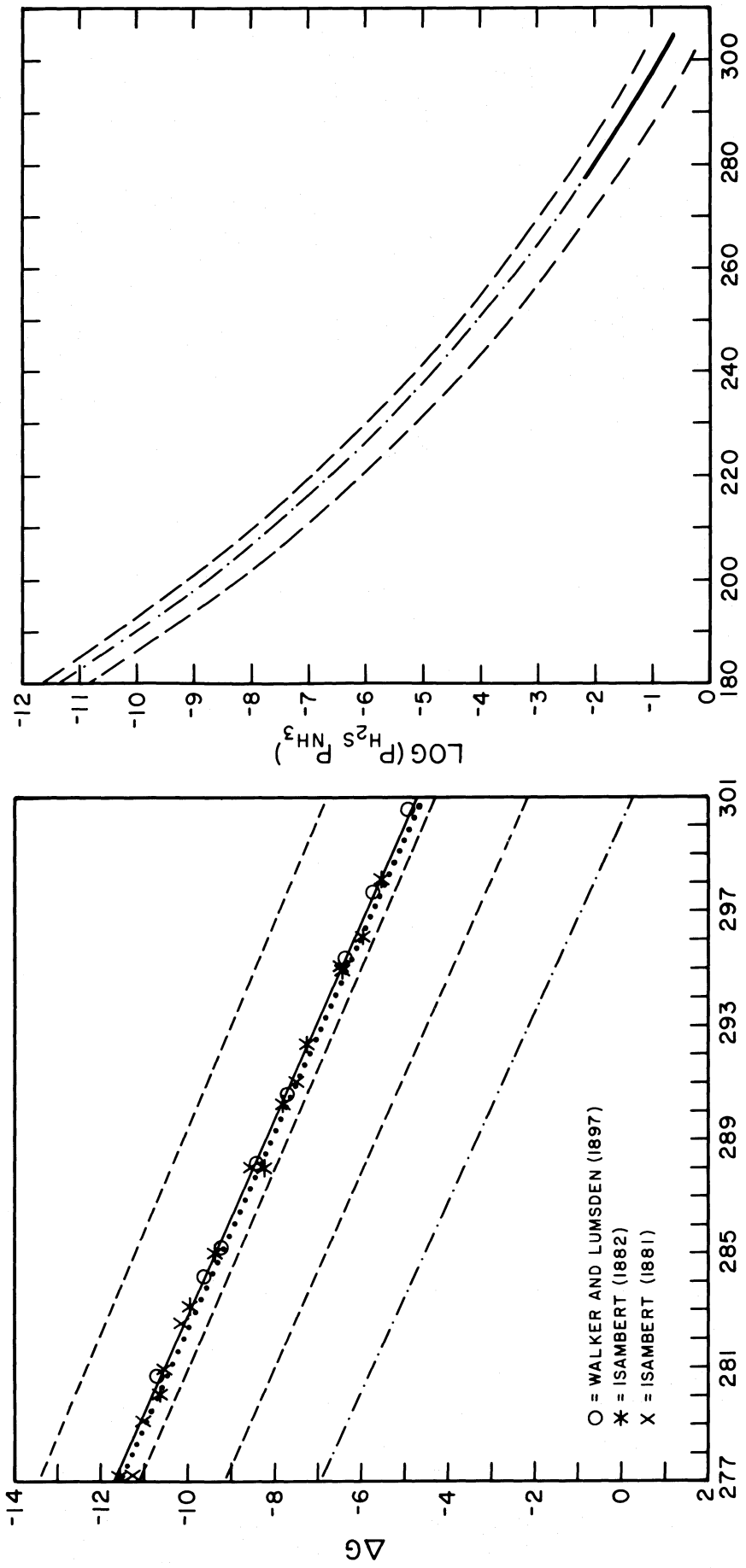

FIG. 4a

FIG. 4b

FIG. 4a.—Change in the Gibbs free energy, ΔG, as a function of temperature for the reaction $NH_3(g) + H_2S(g) \Rightarrow NH_4SH(s)$ derived from published values for the entropy of $NH_4SH(s)$. We used the solid line which represents a fit to the early laboratory data, yielding $S = 115.57$ J deg^{-1} mol^{-1}. The dashed lines show the range in values given by Kelley and King (1961). The dash-dot line corresponds to the value for the entropy given by Wagman *et al.* (1968). The dotted line corresponds to the formula given by Lewis (1969). (*b*) Extrapolation to colder temperatures of the equilibrium constant for the formation of $NH_4SH(s)$. The solid line corresponds to the region of laboratory data shown in Fig. 4*a*; the dash-dot line is its extrapolation. The dashed lines show the range of acceptable values given by Kelley and King (1961).

constant for reaction (4) from the data given in the *Handbook of Chemistry and Physics* (1961).

$$\log k = \log (P_{NH_3} * P_{H_2S}) = 14.82 - (4705/T) . \quad (22)$$

The implied value for the entropy of NH_4SH(s), 116.9 J in excellent agreement with the values derived here).

Further uncertainty is associated with the extrapolation of these data to temperatures much colder than those of the laboratory measurements. The data (Isambert 1881, 1882; Walker and Lumsden 1897) correspond to the temperature range $277 < T < 315$ K, temperatures well above the range of interest on Jupiter. Figure 4*b* shows the extrapolation of the equilibrium constant to colder temperatures, by assuming that differences in the enthalpy (ΔH) and entropy (ΔS) for reaction (4) remain constant over the temperature range. This assumption is equivalent to ignoring the difference in specific heats between NH_3(g) + H_2S(g) and NH_4SH(s) and should produce errors in the equilibrium constant of less than 30% at 200 K. Bragin *et al.* (1977) have recorded the infrared and Raman spectra of NH_4SH(s) over the temperature range 83–390 K. Their data are consistent with the decomposition pressure data (*Handbook of Chemistry and Physics*, 1976; the original reference is Isambert 1881), and they note no phase transitions for NH_4SH with decreasing temperature down to 83 K.

Hydrogen sulfide may condense into H_2S(s) on Jupiter if the volume mixing ratio is above 6×10^{-5} in the upper troposphere. The expression for the saturation vapor pressure (bars) of H_2S(g) above H_2S(s) is given by

$$\log P_{H_2S} = -1329/T + 7.40508 - 0.0051263 * T \quad (23)$$

for the temperature range $164.9 < T < 187.6$ K (Giauque and Blue 1936). Figure 5 shows the temperature dependence of the saturation vapor pressure, where the solid line corresponds to the range of temperature for which equation (23) is validated by laboratory data, and the dashed line represents its extrapolation to colder temperatures, again by assuming constant change in enthalpy and entropy over all temperatures for reaction (5).

The thermodynamic data for the ammonium polysulfide compounds are found only in the NBS publications (e.g., Wagman *et al.* 1968; Rossini *et al.* 1952). These values are particularly uncertain since they refer to aqueous reactions and cannot be traced to laboratory data. The laboratory data of Magnusson (1907) suggest the formation of $(NH_4)_2S$ or the adsorption of NH_3(g) onto the surface of the NH_4SH(s) crystals when NH_3 is at least a factor of 30 more abundant than H_2S. Data for the remaining condensable species, NH_3 and H_2O, were verified with available data on saturation vapor pressures.

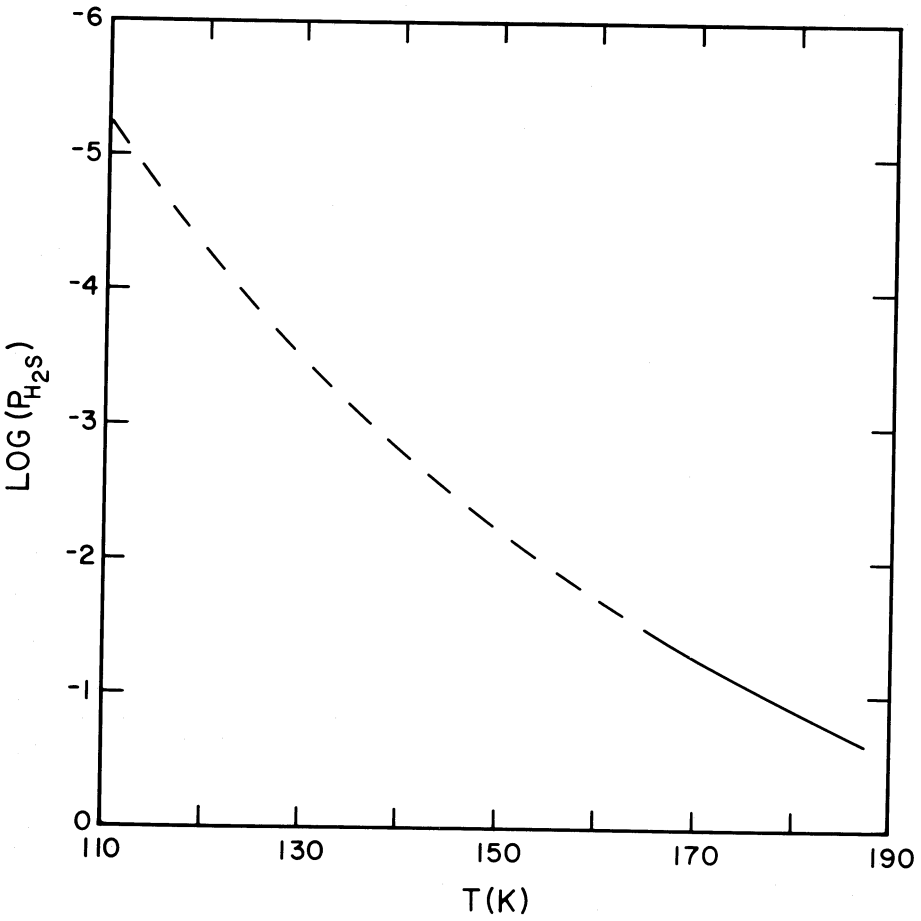

FIG. 5.—Extrapolation to colder temperatures of the saturation vapor pressure of H_2S(g) over H_2S(s). For Jovian applications the vapor pressure formulation must be extended (*dashed line*) beyond the temperature range of the laboratory data (*solid line*).

c) *Atmospheric model*

We use solar composition as a reference case and adopt the pressure-temperature structure derived by Orton (1981). We assume local thermodynamic equilibrium (LTE) at all levels of the atmosphere and no mixing of the condensed phase between levels.

The chemical model calculates the equilibrium composition for each atmospheric level beginning with the gas composition from the level below, cooling the gas according to the *P-T* profile, and removing any condensate. These assumptions are equivalent to assuming that turbulent mixing is sufficiently rapid on small scales so that LTE is maintained between condensate and gas, but not so rapid that it prevents removal of condensates by precipitation or sedimentation during parcel ascent. The primary issue is whether rapid mixing over a length scale, L, with temperature contrast, ΔT, can produce deviations from LTE. Eddy diffusion coefficients have been estimated for Jupiter to be $\sim 10^4$ m^2 s^{-1} (Prinn and Barshay 1977; Stone 1976); sedimentation and precipitation time constants for Jupiter clouds are estimated to vary between 10^2 and 10^4 s (Rossow 1978; Carlson, Rossow, and Orton 1987). Chemical reaction rates are less than 10^2 s at the temperatures and pressures considered. Combining these quantities, together with an approximate temperature lapse rate of 2°C km^{-1}, we estimate that the mixing time constant is comparable to chemical time constants for $L \leq 1$ km and is comparable to the sedimentation and precipitation time constants for $L \approx$ 1–10 km. In the standard model we solve for the gaseous abundances, dissolved gases, dissociation products, and pH at 1 km (2 K) intervals by requiring chemical equilibrium and mass and charge balance.

Difficulty in forming a crystal by vapor condensation, especially in the presence of other aerosols or chemical impurities, leads to the formation of clouds composed of supercooled liquid (Rossow 1978). On Earth water droplets are commonly found to exist at temperatures 15 to 20°C below freezing (Hobbs 1974). The degree of supercooling depends on the background aerosol size and composition, on the chemical composition of the condensed phase, and on the dynamics which control the rate of cooling. Since we do not know these conditions for water clouds on Jupiter, a supercooling of 20°C is chosen for our reference model, along with two extreme cases of 0 and 40°C.

IV. MODEL RESULTS

We present results from the reference calculation in § IV*a* to illustrate the role of aqueous chemical reactions. We then evaluate the effect of uncertainties in the thermodynamic data (§ IV*b*), pressure-temperature profile (§ IV*c*), the effect of the finite step-size (§ IV*d*), and the supercooling of liquid water (§ IV*e*).

a) *Standard Model Results*

The results of our standard model place the water cloud base at 275 K (4.8 bar), allowing aqueous chemistry to occur up to 253 K (3.7 bar). At this point aqueous chemical reactions have depleted the atmospheric abundances of NH_3 and H_2S by 4% and 9%, respectively. The influence of these reactions on the abundances of NH_3 and H_2S is illustrated for the 2 times solar case in Figure 6. The solid lines in the upper panels show the atmospheric partial pressures of NH_3(g) and H_2S(g). It is these partial pressures, not the mixing ratios that drive the aqueous chemistry. Their decrease with altitude is offset by the increased solubilities of NH_3 and H_2S, about a factor of 10 as the temperature decreases from 310 K to 260 K. The ion composition is controlled by the pH of the solution which, for our standard model, ranges from 10 at cloud base to 11 at the cloud top (freezing point). The dominant sulfur species is HS^-, while the NH_3 is equally partitioned between NH_3(a) and NH_4^+. The charge balance in this solution is primarily between NH_4^+ and HS^-, which buffers the solution, keeping the pH relatively low.

Model results for the case where H_2S is not included are denoted by the dashed lines in Figure 6. Large differences are seen in the pH and NH_4^+ concentrations. In the absence of H_2S buffering, charge balance is maintained between NH_4^+ and OH^-, and thus OH^- concentrations increase by more than an order of magnitude. Ammonia is present in this solution predominantly as NH_3(a), and the amount of NH_3 removed by the cloud, NH_3(a) + NH_4^+, is less. The addition of H_2S, therefore, alters the aqueous chemistry by reducing the pH of the solution, increasing the dissolved ammonia, and decreasing the atmospheric abundance of NH_3 at pressures less than 3.7 bar.

The aqueous chemical reactions for our pure H_2O–NH_3 system are the same as those included by empirical formulae in the models of L69 and WL73. Depletion of H_2S by aqueous chemical reactions was included in WL73, again by empirical formula (Leyko 1964), but they did not correctly solve the coupled aqueous system including feedbacks on the dissolved ammonia as discussed above.

Figure 7 summarizes our reference calculations. Methane is not included in this figure, since CH_4 is relatively insoluble in water and its mixing ratio remains constant throughout the lower atmosphere. We have included CO_2 in the standard model at a nominal abundance of 10^{-9}, higher than expected from some thermochemical models, but still an insignificant perturbation to the aqueous chemistry. Aqueous chemical reactions are responsible for reducing the CO_2 abundance from 1×10^{-9} to 5×10^{-11}, thus preventing CO_2 from being the source of the CO observed in the lower stratosphere and upper troposphere. On the other hand, aqueous reactions have no direct effect on the CO abundance. Hence transport of CO directly from the deep atmosphere ($T > 1500$ K) remains the most likely mechanism for maintaining a tropospheric mixing ratio of 10^{-9}. Moreover, if CO_2 were present in the deep atmosphere with a mixing ratio as low as 10^{-12} (Barshay and Lewis 1977), it would not be observable above the water cloud ($< 10^{-13}$). (The identification of regions "above the cloud" must be interpreted with caution since clouds in our model may extend to the tropopause.)

Above the water cloud, the H_2O mixing ratio follows the saturation profile for the vapor over ice. If H_2O is depleted as suggested by Bjoraker, Larson, and Kunde (1986*b*), there would be no aqueous chemistry but water would condense as an ice cloud near 2 bar. An ammonium hydrosulfide cloud forms at 212 K (2.1 bar). Formation of the NH_4SH condensate further depletes the NH_3 mixing ratio by 20% from its value at 3.7 bar and is responsible for the rapid decrease in the H_2S mixing ratio with altitude. As shown in Figure 7, the H_2S mixing ratio decreases from 3.67×10^{-5} to 4×10^{-9} at 1.2 bar, a value well below the current observational upper limit (Larson *et al.* 1984).

Above the ammonium hydrosulfide cloud, the H_2O mixing ratio decreases from 4.3×10^{-9} at 1.2 bar to 4.7×10^{-11} at 0.7 bar and is consistent with the stringent upper limit determined by Larson *et al.* (1984). An ammonia ice cloud forms at 148 K

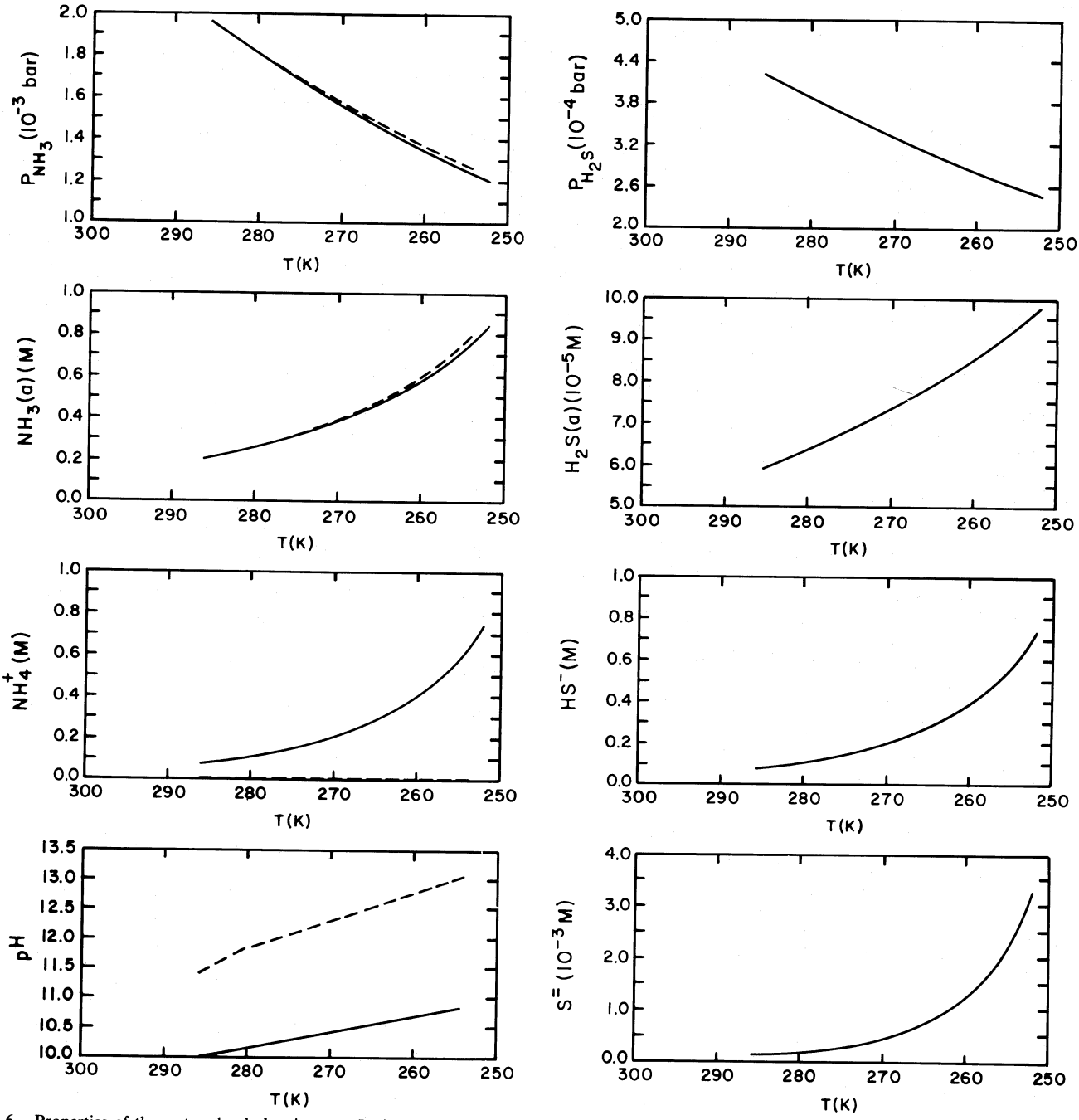

FIG. 6.—Properties of the water cloud chemistry on Jupiter as a function of temperature. A comparison is made between the complete aqueous chemistry determined by the three component system, NH_3–H_2O–H_2S (*solid lines*), and that chemistry without H_2S (*dashed lines*). The partial pressures of NH_3 and H_2S in the atmosphere are shown in the top panels and the molar concentrations of the dissolved (aqueous) gases in the cloud drops, in the panels immediately below. Ionic concentrations of NH_4^+, HS^-, and $S^=$, as well as pH are also included.

(0.68 bar). The ammonia mixing ratio of 1.97×10^{-4} below the cloud base is within the limits imposed by the *Voyager* IRIS and RSS analyses (Kunde *et al.* 1982; Lindal *et al.* 1981). Above this level, the ammonia mixing ratio falls off exponentially following the saturation vapor pressure.

The combined effects of the aqueous chemical reactions and the formation of the NH_4SH condensate are to decrease the bulk abundances of NH_3 by 24% and of H_2S by more than four orders of magnitude. Thus chemical reactions involving H_2O, NH_3, and H_2S within the upper troposphere of Jupiter play an important role in determining the gas composition of the observable atmosphere.

b) Uncertainties in the Thermodynamic Data

As an illustration of the effect of the uncertainties in the thermodynamic data, we consider the case of ammonium hydrosulfides. The uncertainty in the entropy of NH_4SH discussed in § III*b* does not affect the aqueous chemistry, but does alter the location of the NH_4SH(s) cloud base. The upper and lower bounds on the entropy, as given by Kelley and King

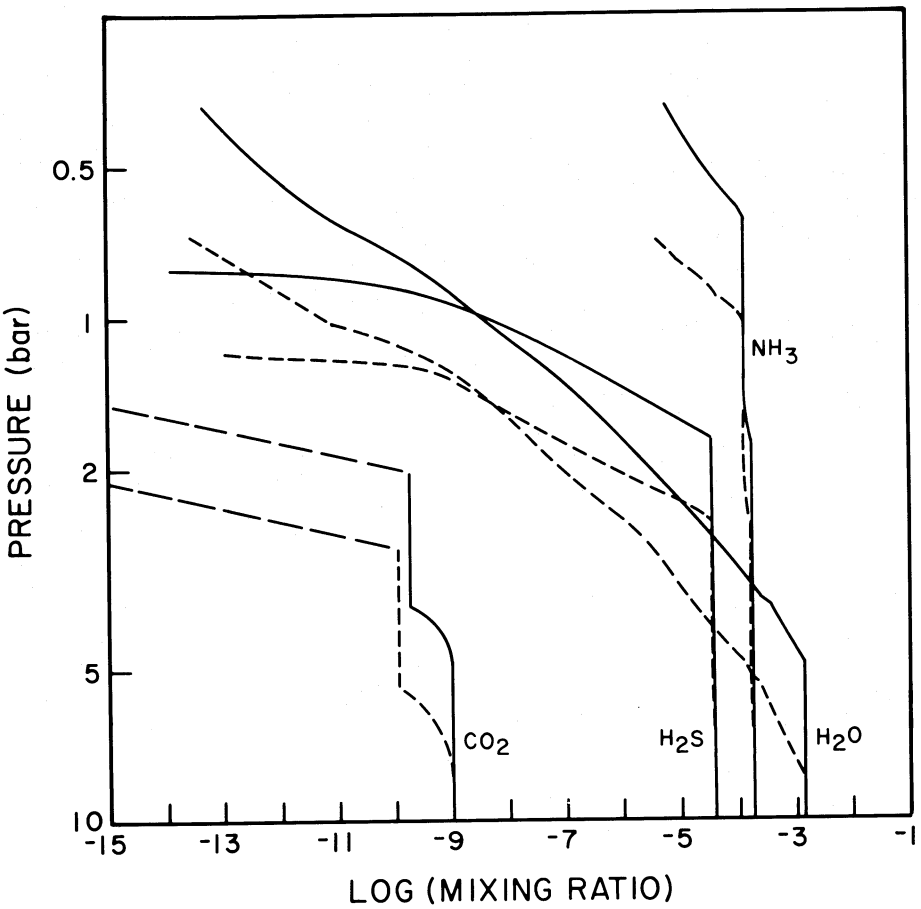

FIG. 7.—Vertical profiles of the mixing ratio of trace gases predicted using the *P-T* profile of Orton (1981, *solid lines*) and profile *b* of Weidenschilling and Lewis (1973, *dashed lines*). Mixing ratio is defined here with respect to H_2. The abundance of species at the lower boundary is from the 1 times solar case as defined in Table 1. Formation of a condensate is indicated by the change in the slope of the mixing ratio profiles. The solubility of CO_2, first in dilute liquid H_2O and then in a NH_3–H_2O slush, is responsible for the decrease above the H_2O cloud base.

(1961) and shown in Figure 4, correspond to a range of 0.3 bar in the predicted cloud location, between 1.8 and 2.1 bar.

The adsorption of NH_3 on NH_4SH(s) or the formation of $(NH_4)_2S$ (Magnusson 1907) are unlikely at NH_3 pressures expected on Jupiter. The reactions that produce polysulfides such as $(NH_4)_2S_2$ are included in this model, but these compounds are very difficult to form since NH_4SH(s) is the preferred form in thermodynamic equilibrium. Likewise, formation of significant amounts of $2NH_3 \cdot H_2O$(s) and $NH_3 \cdot H_2O$(s) are unlikely since the formation of the pure ices, NH_3(s) and H_2O(s) are preferred in thermodynamic equilibrium under Jovian conditions (L69). A large uncertainty in our calculations is due to the extrapolation of gas solubilities to the temperatures of supercooled water. We estimate that these errors should be no larger than 50% in the quantity of dissolved gases at temperatures below 253 K and would have only a small impact on the atmospheric concentrations of NH_3 and H_2S.

c) *Uncertainties in the Pressure-Temperature Profile*

The Orton (1981) profile was derived from an average of the *Voyager* RSS occultation experiment results and may not be representative of conditions at other times or locations. There is no way at present to assess the degree of temporal variability; however, horizontal temperature differences in the uppermost troposphere appear to be of the order of a few °C (Conrath *et al.* 1981; Flasar *et al.* 1981; Gierasch, Conrath, and Magalhaes 1986). Orton (1981) estimated measurement uncertainties to be on the order of ± 2°C for the region probed by the RSS occultation experiment. An additional source of error may be associated with the extrapolation of the profile to levels below where the temperatures are directly retrieved. As an extreme case, we compare the results of our reference model (using the Orton [1981] profile) with those from a model using profile *b* of WL73. The temperature difference between these two profiles is 20°C at the 1 bar level (see Fig. 1). In addition to showing the sensitivity of the model to the adopted profile, this comparison allows us to compare our results directly with those of WL73 as shown in Figure 7. The greatest difference resulting from the use of the WL73 profile (*dashed line*; Fig. 7) is the shift in the cloud bases to much higher pressures. Because the relative humidity is an exponential function of temperature and only a linear function of pressure, the condensate tends to form at about the same temperature in both model atmospheres. For example, the base of the H_2O cloud drops from 4.8 bar (275 K, reference profile) to 8.2 bar (282 K, WL73 profile *b*). Aqueous reactions involving NH_3 and H_2S and the location (in temperature) of the other cloud bases are weakly affected by differences in the thermal profile.

d) Influence of Vertical Resolution

Continuous removal of condensate and LTE are equivalent to assumptions about the turbulent mixing rate, namely that this rate is slower than both the chemical reaction rates and the cloud particle removal rates. Estimates of these time constants, given in § IV, suggest that a 2°C increment is about right. We have also run cases with temperature increments corresponding to vertical scales ranging from 0.25 km to the local pressure-scale height. We find that model results are independent of the temperature increment, excepting the obvious effect on the accuracy of locating the phase change boundaries.

e) Effect of Supercooling

Model calculations were also made with a range of supercooling from 0°C to 40°C. In all instances the H_2O cloud forms at 275 K (4.8 bar). Without supercooling the water freezes at 273 K, and the influence of the aqueous chemistry is negligible. When supercooling persists to 233 K, aqueous-phase reactions continue to lower temperatures and their impact is roughly doubled. With enhanced supercooling, depletion of NH_3 above the water cloud increases from 4% to 7%, while depletion of H_2S increases from 9% to 20%. The formation of the NH_4SH(s) is affected through the reduction of the vapor supply available to form the condensate.

Under Jovian conditions, dissolved gases in the water cloud have only a small effect on the vapor pressure of H_2O, decreasing it by 2% for 20°C supercooling and by 4% in the 40°C case. For the sake of completeness, we have included this depression of the vapor pressure. However, this effect is insignificant when compared with the effects of the phase change: the saturation vapor pressure of H_2O over the solid is less than that over the liquid by 20% at −20°C and by 38% at −40°C. Thus the primary determinant of the abundance of H_2O near the cloud top is the phase of the condensed water.

V. PREFERRED COMPOSITIONS

We have presented a model for Jupiter which includes aqueous chemistry and formation of condensates in the upper troposphere, assuming that equilibrium chemistry approximates the actual trace gas composition between 0.1 and 10 bar. Our analysis indicates that these chemical reactions substantially alter the abundances of trace gases in the upper atmosphere making it difficult to infer bulk composition from current observations. For example, the observation of an NH_3/H_2 ratio at pressures less than 1 bar that is solar or greater requires a bulk abundance of N that is at least 1.5–2 times solar in order to offset the effects of aqueous chemistry and the formation of NH_4SH(s). This conclusion depends on the validity of the assumptions that N/O and N/S ratios are approximately solar. We use results with our preferred composition, 2 times solar, to predict trace gas abundances throughout the upper troposphere, as shown in Figure 8.

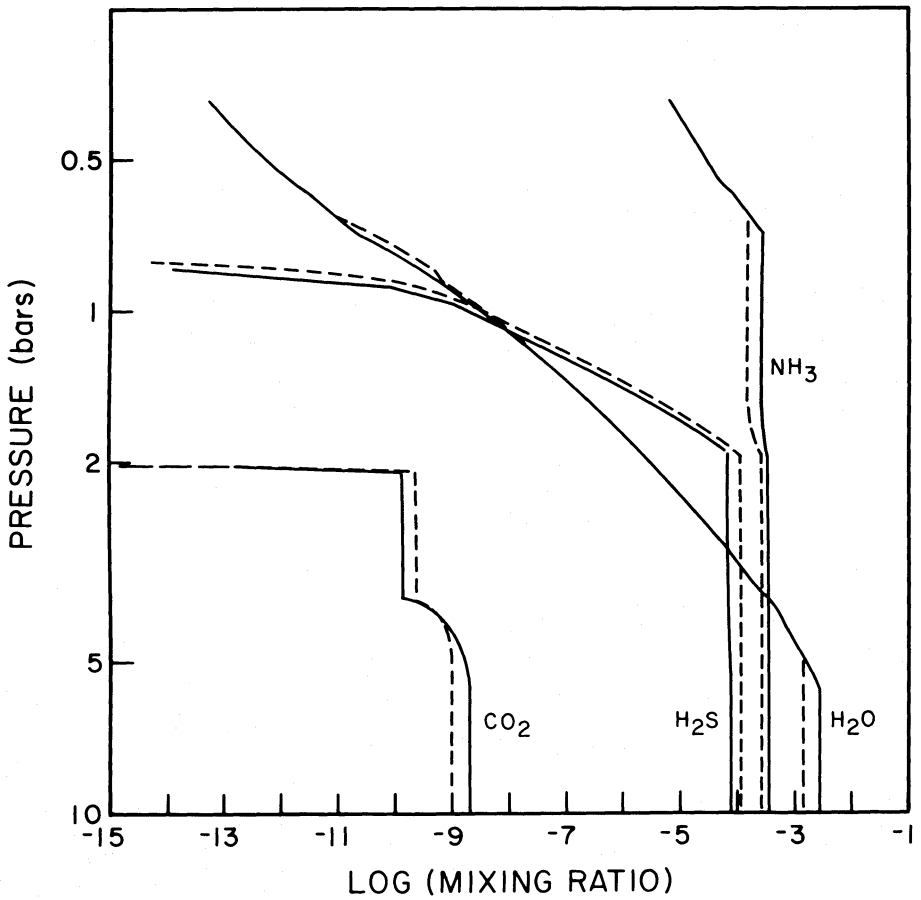

FIG. 8.—Vertical profiles of mixing ratios predicted for our preferred case of 2 times solar (*solid lines*). An alternative composition (*dashed lines*) is shown in order to compare with de Pater (1986). The alternative case has abundances at the lower boundary of 1 times solar H_2O, 1.5 times solar NH_3, and 3 times solar H_2S. Both compositions fit the observations at pressures less than 1 bar.

1. *At and above the base of the NH_3 cloud ($P < 0.7$ bar).*—The NH_3 mixing ratio at the base of the cloud is 2.56×10^{-4}, below the upper limit imposed on the NH_3 abundance at the 1 bar level by Kunde *et al.* (1982). At 0.6 bar the NH_3 abundance has decreased by a factor of 3.5 to 7.3×10^{-5} following saturation. The H_2O abundance in this region of the atmosphere should be controlled by its vapor pressure over the hydrates. Unfortunately, there is no information on the details of the ice hydrates formed in the three-component (NH_3–H_2O–H_2S) system. Based on analogy to the NH_3–H_2O ice system, it is expected that the vapor pressure of H_2O over the ice hydrate in the three-component system would be considerably less than that over the pure ice condensate. For the NH_3–H_2O system, the equilibrium H_2O condensate in this region of the atmosphere is $2NH_3 \cdot H_2O$(s). At the NH_3 cloud base the equilibrium vapor pressure of H_2O above the $2NH_3 \cdot H_2O$(s) hydrate is 1.3×10^{-11} bar, a factor of 4 less than predicted on the basis of pure ice. The abundance of H_2S is less than 10^{-9} throughout this region, although its vapor profile may depend on the type of ice hydrates formed.

2. *Below the NH_3 cloud base and above the NH_4SH cloud base ($0.8 < P < 2.0$ bar).*—In this region the NH_3 abundance decreases from 3.23×10^{-4} at 2.0 bar to 2.56×10^{-4} at 0.8 bar. The H_2S abundance is rapidly depleted from 6.6×10^{-5} to 1×10^{-9} by the formation of NH_4SH(s) condensate. At 1.2 bar the H_2S abundance is already less than 3×10^{-8}, the upper limit imposed by Larson *et al.* (1984). From 1.2 to 2 bar the abundance of H_2O is controlled by its saturation vapor pressure over ice and its mixing ratio decreases with altitude from 2×10^{-6} at 2 bar to 2.9×10^{-8} at 1.2 bar. From 1.2 to 0.8 bar the abundance of H_2O in the atmosphere is controlled first by its vapor pressure over the aqueous solution and then by its vapor pressure over the hydrate ices. Since there is no information on the hydrates in the three-component system there is no way to quantify this dependence. If, as expected, the vapor pressure over the three-component hydrate were less than that over the two-component hydrate, the H_2O mixing ratio would be less than 1×10^{-10} at 0.8 bar. (This value is approximately a factor of 2 less than the vapor pressure over ice.)

3. *Below the NH_4SH cloud base and above the H_2O cloud base ($2.5 < P < 4.5$ bar).*—Aqueous chemical reactions are governed by the pH of the cloud droplets. Ammonia is removed in the predominantly water condensate, and its abundance decreases from 3.48×10^{-4} to 3.23×10^{-4}. The relatively high pH (>10) precludes the dissociation of weaker base species such as PH_3 (*International Critical Tables* 1928). Although the solubility of H_2S(g) is less than that of NH_3(g) in H_2O, the chemical reactions result in a substantial sequestering of sulfides as HS^-(a), and even $S^=$(a) when the pH exceeds 12. The H_2S abundance decreases from 7.53×10^{-5} to 6.7×10^{-5} within this pressure range. The H_2O abundance is controlled by saturation over solution from 4.5 to 3.8 bar and over ice from 3.8 to 2.5 bar. The H_2O/H_2 mixing ratio decreases from 2.76×10^{-3} (2 times solar) at the base of the H_2O cloud to 2.5×10^{-5} at 2.5 bar. We find no chemical mechanisms which can account for the unusual decrease in the H_2O mixing ratio from 6 to 4 bar reported by Bjoraker, Larson, and Kunde (1986*b*).

Our preferred composition is based on the assumption that N/S remains solar. An alternative composition has recently been proposed by de Pater (1986) based on the analysis of Jupiter's radio emission. De Pater reports that the NH_3 abundance decreases from 2.5×10^{-4} (1.4 times solar) at pressures greater than 2 bar to 1.5×10^{-4} at 1.5 bar. On the basis of our model, aqueous chemistry cannot be responsible for the observed depletion NH_3, since at a pressure of 2 bar the temperature is already 65°C below the freezing point of water. A more likely explanation is the formation of NH_4SH(s) with an enhanced abundance of H_2S. To account for the observed NH_3 depletion de Pater suggests an H_2S abundance of 1.75×10^{-4} (5 times solar) at 2 bar. Our best fit to de Pater's observations is with a 3 times solar enhancement of H_2S (1.1×10^{-4}) and a bulk NH_3 abundance of 2.62×10^{-4} (1.5 times solar). The resulting abundance of NH_3 at 1 bar (1.42×10^{-4}) is in conflict with the analysis of the *Voyager* RSS occultation (Lindal *et al.* 1981) but is within the range of acceptable abundances inferred from the *Voyager* IRIS data (Kunde *et al.* 1982); see Figure 8.

VI. DISCUSSION

Observations of methane on Jupiter show a clear enhancement of C/H relative to solar, but enhancement of other elements is still unclear. The bulk abundance of heavy elements (e.g., C, N, O, and S) are constrained only to be less than 10–20 times solar by measurements of the gravitational moments of Jupiter (Stevenson 1982). Available observations of H_2O, NH_3, and H_2S may indicate only lower limits to the abundances of N, O, and S. We use the sensitivity studies with our model to relate N, O, and S to measurements of H_2O, NH_3, and H_2S in the upper troposphere, and to evaluate uncertainties in their inferred abundances.

1. Above the NH_3 cloud base ($P < 0.6$ bar), no effective constraints on N, O, and S can be obtained from measurements since NH_3, H_2S, and H_2O are controlled by their relative humidities and by cloud processes. The relation of the NH_3 abundance near the tropopause to that at deeper levels is further complicated by photochemical destruction (Strobel 1973).

2. Below the NH_3 cloud base and above the NH_4SH cloud base ($0.8 < P < 2.0$ bar), the error committed by interpreting NH_3 abundances to be representative of the bulk abundance N depends on the N/S ratio and on aqueous chemistry. If the N/S ratio is near the solar value, formation of NH_4SH removes 20% of the NH_3. Dynamic effects such as lateral mixing may reduce the relative humidity as in the upper troposphere on Earth. We note that determining the actual abundance of NH_3 in this region would be aided by better measurements of cloud base location and temperature.

3. Below the NH_4SH cloud base and above the H_2O cloud base ($2.5 < P < 4.5$ bar), the N/S ratio can be measured approximately, but only a lower limit can be established for the abundance O. The bulk abundances N and S are different from those measured in this region due to the effects of the water cloud chemistry. The difference is smallest for NH_3, which is depleted by 0%–15% depending on the abundance of H_2O and the magnitude of supercooling. Depletion of H_2S is roughly twice that of NH_3. Thus the bulk abundances of N and S and their ratio could probably be determined to within 10%–20% from measurements in this portion of the atmosphere. A strict test of the assumed sulfur chemistry for Jupiter is provided by measurements of the temperature profile, the location of the NH_4SH cloud base, and the difference in the NH_3 and H_2S mixing ratios between the above-cloud and below-cloud regions. Accurate measurements in this portion of the atmosphere may be obtained only by direct probes,

although remote observations at microwave wavelengths should be pursued. Again, the possible reduction of relative humidities below 100% by large-scale dynamics as on Earth may significantly obscure interpretation of these data.

4. Below the H_2O cloud base ($P > 7$ bar), measurement of the NH_3, H_2O, and H_2S are expected to be directly related to the bulk abundances N, O, and S on Jupiter. We do not expect significant sequestering of these elements in any other compounds (e.g., CO $\ll H_2O$). Nevertheless, if the H_2O abundance is significantly above solar, persistent precipitation may distort abundances below the thermodynamically predicted cloud base (Rossow 1978). Note, for example, that cloud bases on Earth are typically not at the location of thermodynamic equilibrium (i.e., the surface) because of the effects of precipitation and mixing by the large-scale circulation. Thus composition measurements and models may need to be extended to pressures greater than 10 bar to escape the effects expected for the system of massive water clouds on Jupiter. Measurements in this portion of the Jovian atmosphere would require direct probes. Vertical profiles of NH_3, H_2O, and H_2S, as well as CO_2, in the water cloud would provide a direct test of the aqueous chemistry.

This model for the chemistry of the cloud-forming region of Jupiter assumes that microphysical processes within the clouds and large-scale dynamics do not substantially alter the equilibrium abundances. Future efforts should include both chemical and microphysical processes. Such model development is needed to simulate cloud densities and particle size distributions which are critical to the interpretation of observations.

We thank E. Devine for help in preparing the manuscript, L. Del Valle for preparing the figures, and D. Purdy and L. Lawton for bibliographical assistance. This research was carried out while one of us (B. C.) was a NAS/NRC Resident Research Associate at NASA/GSFC/GISS. We would like to acknowledge the support of the Planetary Atmospheres Discipline, NASA Office of Space Science and Applications.

REFERENCES

Barshay, S. S., and Lewis, J. S. 1978, *Icarus*, **33**, 393.
Beer, R. 1975, *Ap. J.*, **200**, L167.
Bézard, B., Marten, A., Baluteau, J. P., Gautier, D., Flaud, J. M., and Camy-Peyret, C. 1983, *Icarus*, **55**, 259.
Bjoraker, G. 1985, Ph.D. dissertation, University of Arizona.
Bjoraker, G. L., Larson, H. P., and Kunde, V. G. 1986*a*, *Icarus*, **66**, 579.
———. 1986*b*, *Ap. J.*, **311**, 1058.
Bragin, J., Diem, M., Guthals, D., and Chang, S. 1977, *J, Chem. Phys.*, **67**, 1247.
Buriez, J. C., and de Bergh, C. 1980, *Astr. Ap.*, **83**, 149.
Cameron, A. G. W. 1982, in *Essays in Nuclear Astrophysics*, ed. C. A. Barnes, D. D. Clayton, and D. N. Schramm (Cambridge: Cambridge University Press), p. 23.
Carlson, B. E., Rossow, W. B., and Orton, G. S. 1987, in preparation.
Conrath, B. J., Flasar, F. M., Pirraglia, J. A., Gierasch, P. J., and Hunt, G. E. 1981, *J. Geophys. Res.*, **86**, 8769.
de Pater, I. 1986, *Icarus*, **68**, 344.
de Pater, I., and Massie, S. T. 1985, *Icarus*, **62**, 143.
Flasar, F. M., Conrath, B. J., Pirraglia, J. A., Clark, P. C., French, R. G., and Gierasch, P. J. 1981, *J. Geophys. Res.*, **86**, 8759.
Gautier, D., Berzard, B., Marten, A., Baluteau, J. P., Scott, N., Chedin, A., Kunde, V., and Hanel, R. 1982, *Ap. J.*, **257**, 901.
Gautier, D., Conrath, B., Hanel, R., Kunde, V., Chedin, A., and Scott, N. 1981, *J. Geophys. Res.*, **86**, 8713.
Gautier, D., and Owen, T. 1983, *Nature*, **304**, 691.
Giauque, W. F., and Blue, R. W. 1936, *J. Am. Chem. Soc.*, **58**, 831.
Gierasch, P. J., Conrath, B. J., and Magalhaes, J. A. 1986, *Icarus*, **67**, 456.
Handbook of Chemistry and Physics. 1983 (Cleveland: Chemical Rubber Publ. Co.).
Handbook of Chemistry and Physics. 1976 (Cleveland: Chemical Rubber Publ. Co.), p. D183.
Handbook of Chemistry and Physics. 1961 (Cleveland: Chemical Rubber Publ. Co.).
Hobbs, P. V. 1974, *Ice Physics* (Oxford: Oxford University Press).
International Critical Tables, 1928 (New York: McGraw-Hill).
Isambert, M. 1881, *C. R. Acad. Sci., Paris*. **92**, 919.
———. 1882, *C. R. Acad. Sci., Paris* **94**, 958.
Kelley, K. K., and King, E. G. 1961, *US Bureau of Mines Bull.*, No. 592.
Kunde, V., *et al.* 1982, *Ap. J.*, **263**, 443.
Larson, H. P., Davis, D. S., Hofmann, R., and Bjoraker, G. L. 1984, *Icarus*, **60**, 621.
Lewis, J. S. 1969, *Icarus*, **10**, 365.
Leyko, J. 1964, *Bull. Acad. Polon. Sci. Ser. Chim.*, **12**, 275.
Lindal, G. F., *et al.* 1981, *J. Geophys. Res.*, **86**, 8721.
Magnusson, J. P. 1907, *J. Phys. Chem.*, **11**, 21.
Martonchik, J. V., Orton, G. S., and Appleby, J. F. 1984, *Appl. Optics*, **23**, 541.
Moroz, V. I., and Cruikshank, D. P. 1969, *J. Atmos. Sci.*, **26**, 865.
Noll, K. S., Knacke, R. F., Geballe, T. R., and Tokunaga, A. T. 1987*a* *Ap. J.*, **309**, L91.
———. 1987*b*, *Ap. J.*, submitted.
Orton, G. S. 1981, *Galileo* Document 1625-125.
Prather, M. J., Logan, J. A., and McElroy, M. B. 1978, *Ap. J.*, **223**, 1072.
Prinn, R. G., and Barshay, S. S. 1977, *Science*, **198**, 1031.
Ridgway, S. T. 1974, *Ap. J.*, (*Letters*), **187**, L41.
Rossini, F., Wagman, D. D., Evans, W. H., Levine, S., and Jaffe, I. 1952, *NBS Circular*, 500.
Rossow, W. B. 1978, *Icarus*, **36**, 1.
Sato, M., and Hansen, J. E. 1979, *J. Atmos. Sci.*, **36**, 1133.
Schaaf, J. W., and Williams, D. 1973, *J. Opt. Soc. Am.*, **63**, 726.
Stevenson, D. J. 1982, *Planet. Space Sci.*, **30**, 755.
Stone, P. H. 1976, in *Jupiter*, ed. T. Gehrels (Tucson: University of Arizona Press), p. 586.
Strobel, D. F. 1973, *J. Atmos. Sci.*, **30**, 1205.
Strobel, D. F., and Yung, Y. L. 1979, *Icarus*, **37**, 256.
Stull, D. R., and Prophet, H. 1971, *JANAF Thermochemical Tables* (NSRDS-NBS-37), 2d ed.
Stumm, W., and Morgan, J. J. 1981, *Aquatic Chemistry: An Introduction Emphasizing Chemical Equilibria in Natural Waters*, (2d ed.; New York: Wiley).
Wagman, D. D., Evans, W. H., Parker, V. B., Halow, I., Baily, S. M., and Schumm, R. H. 1968, *NBS Tech Note*, 270-3
Walker, J., and Lumsden, J. S. 1897, *J. Chem. Soc. London*, **71**, 428.
Weidenschilling, S. J., and Lewis, J. S. 1973, *Icarus*, **20**, 465.
West, R. A., Strobel, D. F., and Tomasko, M. G. 1986, *Icarus*, **65**, 161.

Note added in proof.—We have recently received a preprint of Fegley and Prinn (1988, *Ap. J.*, in press). This work examines the implications of the subsolar H_2O abundance (Bjoraker, Larson, and Kunde 1986*b*) for the abundances of the nonequilibrium trace gases CO and SiH_4. Based on their model calculations, Fegley and Prinn (1988) conclude, as we do, that the observed abundance of CO ($\sim 10^{-9}$) is incompatible with the significant global water and oxygen depletions implied by the Bjoraker, Larson, and Kunde (1986*b*) analysis.

BARBARA E. CARLSON, MICHAEL J. PRATHER, and WILLIAM B. ROSSOW: NASA/GISS, 2880 Broadway, New York, N.Y. 10025